Soils and Rocks
An International Journal of Geotechnical and Geoenvironmental Engineering
www.soilsandrocks.com
ISSN 1980-9743
ISSN-e 2675-5475

Experimental study on mechanical behavior deterioration of undisturbed loess considering freeze-thaw action

Shuangshuang Yang[1], Yaling Chou[1#], Lijie Wang[1], Peng Zhang[1]

Article

Keywords
Freeze-thaw action
Undisturbed loess
Triaxial shear test
Failure form
Stress-strain curve

Abstract

To solve the problem that the mechanical behavior of undisturbed loess in seasonally frozen soil area is affected by freeze-thaw action, triaxial shear tests of undisturbed loess under freeze-thaw condition were carried out. The results show that the mechanical properties of undisturbed loess are greatly affected by factors including freeze-thaw process, water content, natural density and confining pressure. Freeze-thaw action has a certain impact on the failure surface shape and stress-strain curve. Before and after freeze-thaw, the shape of the shear failure surface is complex, including single oblique failure surface, double oblique failure surface, vertical failure surface, X-shaped failure surface, bulging failure, etc. And under the conditions of low water content, low confining pressure and high dry density, the stress-strain curve tends to be softened. Conversely, the curve tends to harden. Freeze-thaw action can make the stress-strain curve transition from softening to hardening. In addition, the freeze-thaw action significantly weakens the failure strength, shear strength, cohesion, initial tangent modulus and failure ratio of undisturbed soil, but does not change the internal friction angle obviously. Also, the heterogeneity of natural soil is also an important factor affecting the mechanical parameters, failure surface shape and stress-strain curve of undisturbed loess.

1. Introduction

Freeze-thaw action of soil is an important research topic in mechanics of frozen ground. It has been found that freezing-thawing can change the permeability, bulk density, water content, strength parameters, etc. of soil (Chamberlain & Gow, 1979; Ma et al., 1999; Qi et al., 2003; Yang et al., 2003; Wang et al., 2007; Ye et al., 2012; Fang et al., 2012). These changes are due to the fact that freeze-thaw action changes the original structure of the soil, namely destroys the connection force and arrangement relationship among the soil particles (Konrad, 1989). Especially in the seasonally frozen soil area covered by loess in the northwest, China, the freeze-thaw cycle, as a kind of strong weathering process, repeatedly changes the microstructure and physical properties of the loess, which in turn strongly affects the engineering mechanical behavior of the loess, leading to deterioration in the strength of the soil and even causing destabilization damage to infrastructures such as roads, airports and underground pipelines in severe cases.

At present, there are many literatures about the effects of freeze-thaw cycle on physical and mechanical properties of loess. Hu et al. (2014) investigated the strength of remolded Yangling loess in China under freeze-thaw cycles. Wei et al. (2018) studied the influence rule of freezing temperature on the mechanical properties of remolded loess. Song et al. (2008) studied that freeze-thaw cycles had the dual effects of strengthening and weakening on remolded loess with different dry weights. Ni & Shi (2014) studied the effect of freeze-thaw cycles on the microstructure and strength of remolded loess. Wang et al. (2010) researched the influence of freeze-thaw on cohesion and internal friction angle of remolded loess. Ye et al. (2018) obtained the fitting formula among the number of freeze-thaw cycles, water content and cohesion of undisturbed loess through experiments. Dong et al. (2010a, b) found that after 3~5 freeze-thaw cycles, the cohesion of remolded loess decreased to a minimum, and the internal friction angle did not change much. Xu et al. (2016) studied the effects of freeze-thaw action on the microstructure and strength of undisturbed loess. Li et al. (2020) studied the influence of freeze-thaw action on the shear strength of undisturbed loess.

Above all, rich research results have been obtained on the effect of freeze-thaw on loess, but most of them are

#Corresponding author. E-mail address: chouyaling@lzb.ac.cn
[1]Lanzhou University of Technology, Key Laboratory of Disaster Prevention and Mitigation in Civil Engineering of Gansu Province, Lanzhou, Gansu, China.

Submitted on June 5, 2022; Final Acceptance on September 29, 2023; Discussion open until May 31, 2024.
https://doi.org/10.28927/SR.2024.005822

for remolded soils. Due to the heterogeneity of undisturbed loess, there are no undisturbed soils with exactly the same water content, natural density and other physical indicators. In fact, there is a fundamental difference in the mechanical behavior between undisturbed soil and remolded soil (Bjerrum, 1967; Burland, 1990). However, when carrying out engineering design in seasonally frozen areas, the disturbed soil indicators are often simply used, without considering the difference between the physical and mechanical properties of the undisturbed soil before and after freeze-thaw. And this simplified treatment method is not consistent with the actual project, mainly because of the lack of relevant measured data in this field. However, there are many engineering projects involving undisturbed loess in the seasonally frozen soil area covered by loess in western China. Therefore, this article carries out the undisturbed loess considering freeze-thaw.

2. Materials and methods

Undisturbed loess, from Lanzhou of China, is used in the experiment. The soil samples are taken from the foundation pit of a high-rise building in Pengjiaping, Lanzhou City, and the depth of obtaining soil is between 6.0 m and 7.0 m below ground level. The sampling method of soil samples is as follows: Firstly, cut out cubes with a bottom size of about 16 cm × 16 cm and a height of about 30 cm with a cutter along the side wall at the bottom of the foundation pit; Then, cut off the edges and corners and both ends and put them into the self-made iron-sheet sampling buckets (15 cm × 15 cm × 25 cm); Finally, cover them with lids and seal them with transparent tapes (to prevent water from evaporation) and bring them back to the laboratory. Eventually, the size of undisturbed soil samples obtained by manual cutting method is Φ61.8 mm × 125 mm (tri-axial test soil specimen). The soil cut down during the preparation of the undisturbed soil sample is air-dried, crushed, and then passes through a sieve of 2 mm to test the basic physical properties of the soil. The soil sample under the sieve is taken and mixed thoroughly to determine the particle analysis curve as shown in Figure 1. The specific gravity of soil particle is 2.72, the natural water content is between 4.22% ~ 18.22% (The water content of the soil varies greatly in different directions around the foundation pit, and taking this into account, soil samples with different water content were obtained in different directions), the natural density is between 1.52 ~ 1.79 g/cm^3, the liquid limit is 24.9%, the plastic limit is 15.7%, and the plasticity index is 8.2. The first freeze-thaw cycle has the greatest effect on the properties of soil (Wang et al., 2005), and the strength reaches stability after 3 ~ 5 freeze-thaw cycles (Dong et al., 2010a, b). Therefore, the number of freeze-thaw cycles in this experiment is mainly set as 1 time, and the number of freeze-thaw cycles of a few soil samples is set as 3 times for comparison. The lowest daily mean air temperature in Lanzhou can reach -10 °C. Taking into account the warming effect of the boundary layer (Zhu, 1988) and the exponential decay of ground temperature amplitude with the increase of depth (Xu et al., 2001), the freezing environment temperature of soil samples is set to -1 °C and -5 °C respectively in laboratory experiments. Soil samples are frozen for 12 hours and thawed at room temperature (17-20 °C) for 12 hours, which is named one freeze-thaw cycle. During the freezing-thawing process, the samples are all in a closed state (soil samples are sealed with a plastic bag to prevent water from dispersing), without water replenishment. The soil samples have been freeze-thawed in the thermostatic refrigerator before they are installed in the triaxial shear apparatus. The unconsolidated-undrained (UU) triaxial shear test is carried out. The shear rate is set to 0.8 mm/s.

A total of 112 undisturbed soil samples are designed for the experiment. During obtaining undisturbed soil samples in the field, considering that the soil samples may be damaged in the process of transportation, sample preparation and experiment, or some soil samples may not meet the experimental requirements, a total of 130 soil samples are collected by iron bucket. In experiment process, some data are abnormal or incomplete due to sample preparation failure, equipment failure, or a few soil samples fail to meet the experimental requirements influenced by the initial structure, so they are eliminated (as shown in Table 1 and Table 2). Since the natural water contents and natural densities of the undisturbed soils are different, the standard for sample grouping is to group the samples with relatively close natural water contents into one group. Table 1 and Table 2 show the experimental design of undisturbed soil samples without freeze-thaw and after one or three freeze-thaw cycles, respectively. Under the same experiment conditions, the soil samples that the average difference of water content and density between freeze-thaw soil samples and no freeze-thaw soil samples respectively does not exceed 1.5% (except for the soil sample of F3 group

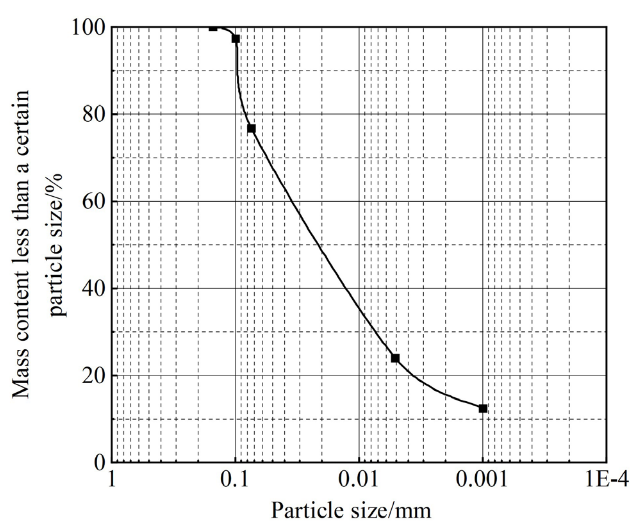

Figure 1. Particle analysis curve.

Table 1. Experiment design of undisturbed soil without freeze-thaw and after one freeze-thaw cycle.

Sample number		Confining pressure Natural density	Experiment condition			
			Water content	Number of freeze-thaw	Freezing temperature	
(N)		(kPa)	(g·cm^{-3})	(%)	(n)	(°C)
G1	I-1	100	1.70/1.65	4.22/4.55	1	-5
	I-2	200	1.72/1.68	4.60/4.67	1	-5
	I-3	300	1.73/1.76	4.36/4.29	1	-5
	I-4	400	1.69/1.62	4.72/5.78	1	-5 (eliminate)
	I-5	500	1.67/1.60	4.61/6.12	1	-5 (eliminate)
G2	II-1	100	1.79/1.72	6.62/7.93	1	-5
	II-2	200	1.70/1.69	7.66/8.23	1	-5
	II-3	300	1.68/1.62	8.55/8.95	1	-5
	II-4	400	1.73/1.76	8.94/9.43	1	-5
	II-5	500	1.64/1.69	9.26/9.98	1	-5
	II-6	600	1.62/1.56	9.29/12.9	1	-5
G3	III-1	100	1.59/1.63	16.20/15.91	1	-5
	III-2	200	1.60/1.65	17.91/18.02	1	-5
	III-3	300	1.72/1.62	16.41/17.42	1	-5
	III-4	400	1.73/1.67	15.42/16.90	1	-5
	III-5	500	1.62/1.58	14.70/15.21	1	-5
	III-6	600	1.52/1.59	18.22/18.13	1	-5(eliminate)

Note: In front of the oblique line are the water content and density of soils before freeze-thaw, and behind the oblique line are the water content and density of soil samples after one freeze-thaw cycle.

Table 2. Experiment design of undisturbed soil without freeze-thaw and after three freeze-thaw cycles.

Sample number		Confining pressure Natural density	Experiment condition			
			Water content	Number of freezing and thawing	Freezing temperature	
(N)		(kPa)	(g·cm^{-3})	(%)	(n)	(°C)
F1	I-1	100	1.68/1.72	12.83/13.72	3	-1
	I-2	200	1.62/1.65	14.61/13.21	3	-1
	I-3	300	1.69/1.66	15.81/13.74	3	-1
	I-4	400	1.72/1.63	12.84/14.22	3	-1 (eliminate)
	I-5	500	1.70/1.72	13.28/15.06	3	-1 (eliminate)
F2	II-1	100	1.52/1.62	11.71/12.96	3	-5
	II-2	200	1.69/1.54	9.97/11.46	3	-5
	II-3	300	1.60/1.60	14.26/13.73	3	-5
	II-4	400	1.74/1.52	9.99/12.27	3	-5
	II-5	500	1.67/1.70	10.42/12.55	3	-5 (eliminate)
F3	III-1	100	1.65/1.65/1.70	14.21/14.43/16.67	3、1	-1
	III-2	200	1.69/1.74/1.64	13.92/13.36/15.96	3、1	-1
	III-3	300	1.70/1.70/1.69	14.51/14.23/17.73	3、1	-1
	III-4	400	1.72/1.69/1.73	13.44/13.59/16.85	3、1	-1
	III-5	500	1.70/1.79/1.67	13.36/14.56/16.56	3、1	-1 (eliminate)
F4	IV-1	100	1.69/1.65	8.75/9.23	3	-1
	IV-2	200	1.71/1.69	9.39/9.76	3	-1 (eliminate)
	IV-3	300	1.74/1.72	9.56/8.98	3	-1
	IV-4	400	1.68/1.64	7.39/8.77	3	-1

Note: Before and after the oblique line are the water content and density of the soils before freeze-thaw and after three freeze-thaw cycles, respectively. For F3, behind the second oblique line are the water content and density of soil samples after one freeze-thaw cycle.

with one freeze-thaw cycle, the average difference of water content of other soil samples in the same group does not exceed 1.5%) and 0.10 g/cm^3 are selected for experiment (previous studies have shown that water content have a significant impact on soil, so soil samples with relatively close water contents are grouped into one group).

3. Analysis and results

3.1 Failure form of soil sample

Freeze-thaw cycles change the properties of the soil and make the soil into a new stable equilibrium state (Yang et al., 2003). The height, diameter and water content of the soil samples before and after freeze-thaw are measured, respectively. It is found that the water content does not change much before and after freeze-thaw, fluctuating generally between 0 and 0.09%. The height change of the sample does not exceed 0.6 cm, and the diameter change does not exceed 0.3 cm. Under shear loading, the undisturbed soil samples are often damaged along the weakness planes until they are destroyed, thus forming the distinct shear surface. Figure 2 shows the preparation process of undisturbed soil and the soil samples after shear failure.

Since the experiment object is undisturbed soil, the failure surface form is more complicated due to the influence of the heterogeneity of natural soil. Freeze-thaw action has a certain impact on the failure surface shape, and the water content, dry density and confining pressure have a greater effect on the failure surface form of soil samples. Before and after freeze-thaw, the shape of the shear failure surface is complex, including single oblique failure surface, double oblique failure surface, vertical failure surface, X-shaped failure surface, bulging failure, as shown in Figure 3.

1. Single oblique failure surface: After shear failure, an oblique failure surface runs through the side of top of the soil sample to the other side of the bottom of the soil sample, as shown in Figure 3e, Figure 3f and Figure 3g. This failure surface is roughly 60° ~ 65°, and most of the soil samples belong to this condition. It is estimated that the internal friction angle of undisturbed loess is mainly concentrated between 30° and 40°. Soil samples with high water content and natural density and relatively uniform soil quality are prone to this kind of failure.
2. Double oblique failure surface: After shear failure, two nearly parallel failure surfaces are generated, as shown in Figure 3d. This failure surface is roughly 60° ~ 65°. This failure form is not so much in this experiment, there are 3 cases in total, and it mainly appears in soil samples with medium water content.
3. Vertical failure surface: For soil samples with lower natural density, lower water content and lower initial confining pressure, or soil samples with vertical micro-cracks, deviatoric stress plays a role similar to splitting during failure, and the failure surface shows cracks close to vertical direction or partly close to vertical direction, as shown in Figure 3a and Figure 3c.
4. X-shaped failure surface: After shear failure, a set of cross-conjugate symmetric failure surfaces appear, as shown in Figure 3h. This situation mainly occurs in the soil samples with higher water content, higher natural density, more uniform structure and higher sample preparation accuracy.
5. Bulging failure: As the failure form in Figure 3b, in the case of lower density, higher water content and higher confining pressure, the samples are compressed with gradual increase of axial deformation, and the outward bulging phenomenon appears in the middle of the soil sample. This phenomenon is called lateral bulging failure, obvious shear surface does not appear, and peak value does not appear in the stress-strain curve.

3.2 Stress-strain relationship of soil

The stress-strain relationship curve is the basis for studying the mechanical properties of soil. Figure 4 shows the stress-strain relationship curve of undisturbed loess sample without freeze-thaw. The stress-strain curve of undisturbed loess varies with water content, sedimentary age and stress state, generally presenting three types and five forms: brittle failure type (strong softening and weak softening), plastic failure type (strong hardening and weak hardening) and ideal plastic failure type (Liu, 1997). It can be seen that the stress-strain relationship curves of undisturbed loess without freeze-thaw are mainly brittle failure type (Figure 4a) and plastic failure type (Figure 4b). Brittle failure mainly occurs in soil samples with relatively low water content and high dry density, and the stress-strain curve shows a strain-softening type with high failure peak and small failure strain. The stress-strain curve is divided into four stages: (1) Linear elasticity stage: in the initial stage of the experiment, the stress increases linearly with the strain; (2) Strengthening stage: the strength increases continuously with the increase of the load, the curve deviates from the linearity, and the stress increases with the increase of the deformation and finally reaches the peak strength; (3) Softening stage: after the strength reaches the peak value, the shear resistance gradually loses, and the stress-strain curve presents as a non-linear monotonic decreasing. At this stage, slippage occurs among the soil particles, shear zone is gradually generated, and dilatancy phenomenon occurs until it reaches residual strength; (4) Flow stage: After reaching the residual strength, the stress-strain curve tends to a straight line, and the strain increases continuously under the condition of constant stress, that is, the soil sample is completely destroyed.

When the water content is higher and the dry density is lower, the shear failure changes from brittle failure to

Figure 2. The preparation process of undisturbed soil and the soil samples after shear failure.

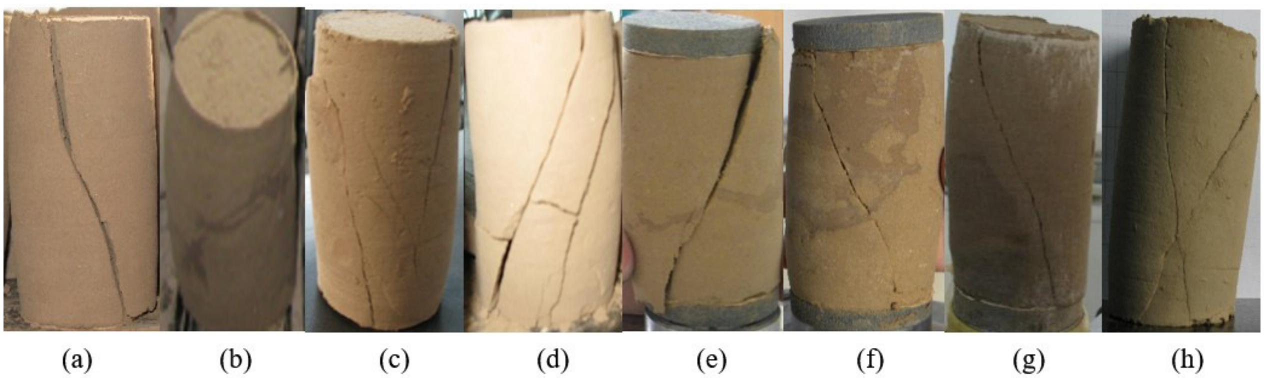

Figure 3. Shear failure surfaces of different undisturbed soil samples before and after freeze-thaw: (a) vertical failure surface; (b) bulging failure; (c) vertical failure surface; (d) double oblique failure surface; (e) single oblique failure surface; (f) single oblique failure surface; (g) single oblique failure surface; (h) X-shaped failure surface.

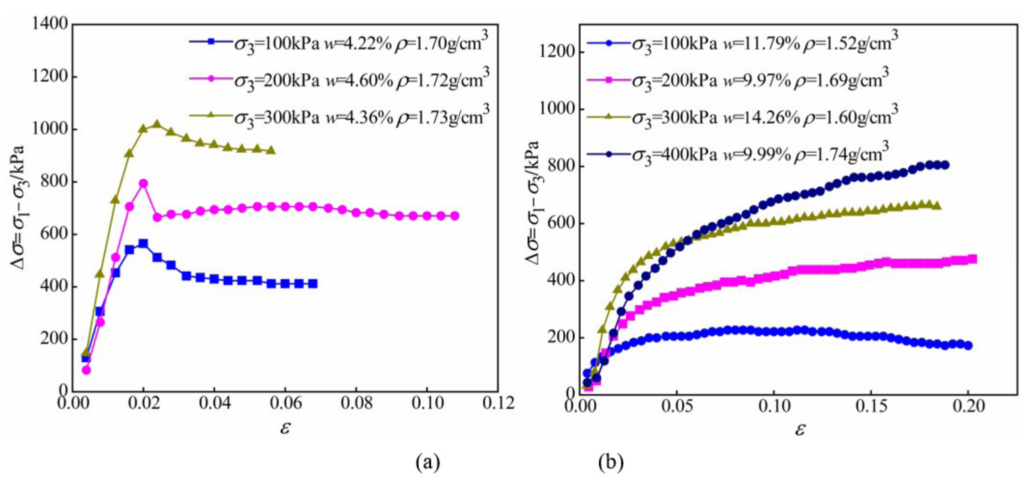

Figure 4. Stress-strain curve of undisturbed loess sample without freeze-thaw: (a) brittle failure type (G1 soil sample); (b) plastic failure type (F2 soil sample).

plastic failure. After the shear stress reaches the yield point, it changes from elastic deformation to plastic hardening, the shear stress releases slowly, and the stress-strain curve shows a hardening type. With the increase of confining pressure, the stress-strain curve gradually changes from weak hardening type to strong hardening type. When the confining pressure is lower, the stress-strain curve shows the softening type or the weak hardening type. On the contrary, when the confining pressure is higher, the soil structure is partially destroyed in the consolidation process, and the stress-strain curve shows a strong hardening type.

Figure 5 shows the stress-strain curves of undisturbed loess under different confining pressures without freeze-thaw. Herein, the similarities and differences of stress-strain curves of soil samples with different water contents under the same confining pressure are analyzed. As the confining pressure increases, the strength of the soil sample increases, and the type of stress-strain curve of the samples with different water contents changes. Under the same confining pressure, although there are differences among soil sample densities, the influence of water content on the stress-strain curve is significant. For soil samples with water content of about 4%, the stress-strain curves show obvious post-peak softening. With the increase of water content, the stress-strain curve gradually changes from strong softening type to hardening type. With the increase of confining pressure, the stress-strain curve of soil samples with water content between 6% and 11% changes from weak softening type to weak hardening type, and then to strong hardening type. And for soil samples with water content greater than 14%, the stress-strain curve basically shows the strong hardening type. In addition, for a few individual soil samples, the stress-strain curve basically shows an ideal plastic failure type.

Figure 6 shows the stress-strain curve of the soil samples before and after freeze-thaw cycles. In Figure 6a, the number of freeze-thaw cycles of G1 soil sample is once, and the peak strength decreases significantly after freeze-thaw, as well as the initial tangent modulus and residual strength. The number of freeze-thaw cycles of G2 soil samples in Figure 6c and G3 soil samples in Figure 6d are both once. When the confining pressure is 100 kPa, the stress-strain curve before and after freeze-thaw shows a weak softening type. With the increase of confining pressure, the stress-strain curves are all strain hardening. Under the same confining pressure, the stress-strain curve of soil samples after freeze-thaw is always lower than that of the corresponding soil samples before freeze-thaw, which indicates that the freezing-thawing process weakens the peak strength, failure strength and residual strength of undisturbed soil. In Figure 6b, the number of freeze-thaw cycles of F2 soil sample is three times, and the influence of

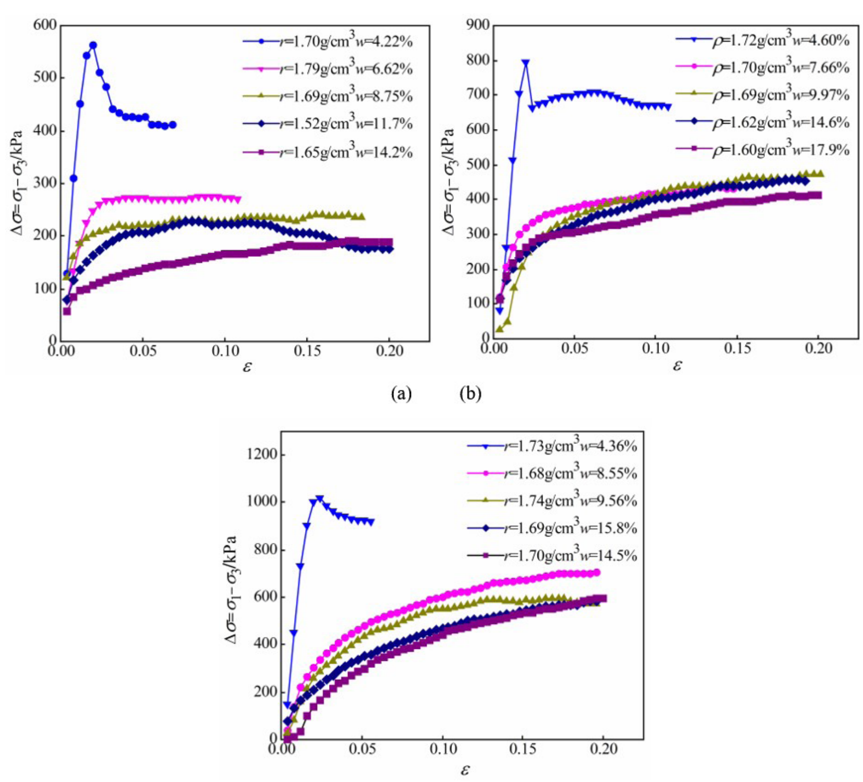

Figure 5. The stress-strain relation curves of undisturbed loess without freeze-thaw under different initial conditions: (a) confining pressure 100 kPa (G1 G2 F2 F3 F4); (b) confining pressure 200 kPa (G1 G2 G3 F1 F2); (c) confining pressure 300 kPa (G1 G2 F1 F3 F4).

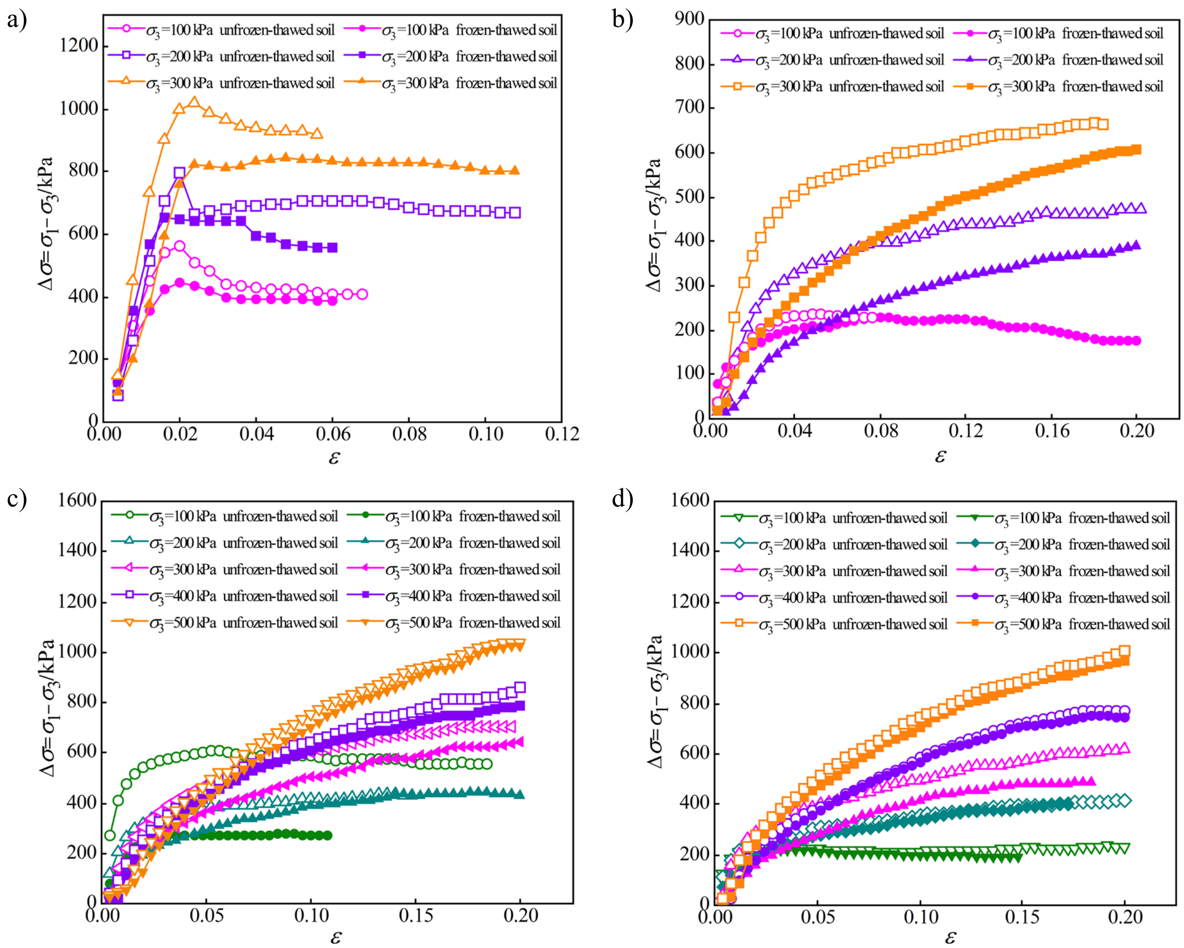

Figure 6. The stress-strain relationship curves of soil samples before and after freeze-thaw cycle: (a) soil sample G1 (freeze-thaw 1 time); (b) soil sample F2 (freeze-thaw 3 times); (c) soil sample G2 (freeze-thaw 1 time); (d) soil sample G3 (freeze-thaw 1 time).

Note: "unfrozen-thawed soil" in Figure 6 represents"soil before freeze-thaw", and "frozen-thawed soil" represents "soil after freeze-thaw".

confining pressure and freeze-thaw on stress-strain curves is similar to G2 and G3. Under the same confining pressure, the deviatoric stress of soils after three freeze-thaw cycles is obviously smaller than that of soil samples without freeze-thaw.

Figure 6 has shown the freeze-thaw action significantly deteriorates the failure strength of the undisturbed loess, and the failure deviatoric stress is significantly reduced, which is consistent with the research results of the literature (She et al., 2020; Xu et al., 2020). The lower the water content and the higher the dry density of soil samples, the higher the strength, the more obvious the decay of failure strength after freeze-thaw, and the greater the difference between the peak strength of stress-strain curve before and after freeze-thaw. For soil samples with high water content and low dry density, the failure strength decreases a little after freeze-thaw cycle. In terms of the number of freeze-thaw cycles, after three freeze-thaw cycles, the difference between the stress-strain curves of soil samples before and after freeze-thaw cycles is larger. The stress-strain curves of the soil samples with low water contents after freeze-thaw still show a post-peak softening type, but due to the significant reduction of natural strength, the stress-strain curves have a transition trend from strong softening to weak softening. After freeze-thaw, the stress-strain curve of the undisturbed soil with high water content has a transition trend from weak softening to weak hardening or from weak hardening to strong hardening. Before and after freeze-thaw, the stress-strain curve tends to be softening type under low water content, low confining pressure and high dry density. Otherwise, the curve tends to be hardening type. Freeze-thaw action has a certain impact on the stress-strain curve, and it can make the curve transition from softening to hardening.

3.3 Strength parameter

According to the triaxial shear test, the axial stress σ_1 and the lateral stress σ_3 (i.e., confining pressure) can be measured. Based on the *p*-*q* coordinate system, the corresponding deviatoric stress *p* and spherical stress *q* are respectively:

$$p = \left(\sigma_1 + \sigma_3\right) / 2 \tag{1}$$

$$q = \left(\sigma_1 - \sigma_3\right)/2 \quad (2)$$

Herein, the maximum principal stress difference $(\sigma_1\text{-}\sigma_3)_{max}$ is taken as the failure criterion. When there is no peak value in the stress-strain curve, the principal stress difference corresponding to 14% of the axial strain is taken as the shear strength. On this basis, the strength envelop of soil sample is drawn in the coordinate plane. All the experimental soil sample data were fitted by based on the coordinate algorithm. But there is too much data, due to space limitations, this article only has listed one of the soil samples in Figure 7 (G2 samples). It can be seen that the fitting is good (the correlation coefficients are higher than 0.98). The intercept of the strength envelope line with the q axis is the α value, and the inclination angle with the p axis is α value. Equations 3 and 4 are used to calculate the internal friction angle φ and cohesion c of the soil samples respectively, as shown in Table 3.

$$\varphi = \sin^{-1}\left(\tan\alpha\right) \quad (3)$$

$$c = \frac{a}{\cos\varphi} \quad (4)$$

From Table 3, it can be seen that the attenuation of undisturbed soil strength is mainly due to freeze-thaw action. For strength parameters, the lower the water content, the more obvious the strength damage and the greater the cohesion reduction of

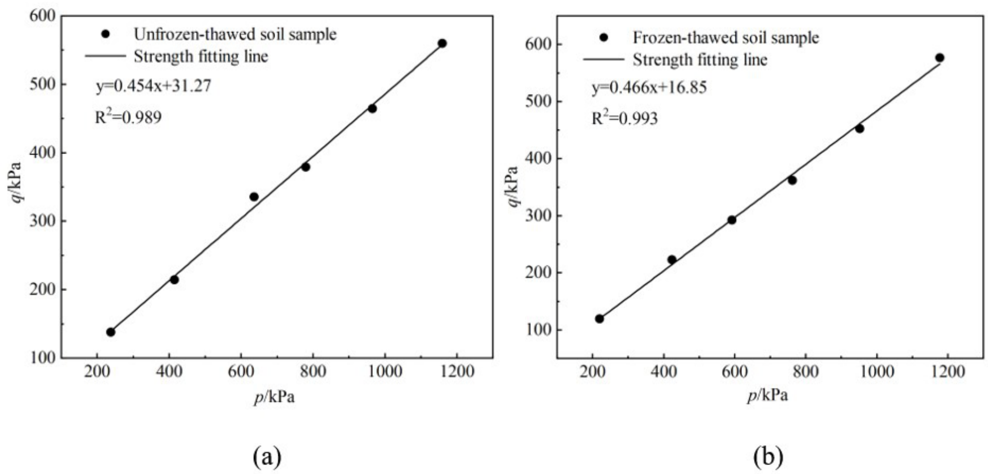

Figure 7. Strength envelop for G2 samples before and after freeze-thaw: (a) unfrozen-thawed soil sample; (b) frozen-thawed soil sample.
Note: "unfrozen-thawed soil" in Figure 7 represents "sample before freeze-thaw", and "frozen-thawed soil" represents "sample after freeze-thaw".

Table 3. The strength parameters of soil samples calculated by p-q coordinate system.

Sample number	Number of freeze-thaw	Freezing temperature	Average water content	Average density	Internal friction angle φ	Cohesion c
(N)	(time)	(°C)	(%)	(g·cm^{-3})	(°)	(kPa)
G1	0	—	4.39	1.72	27.7	123.2
	1	-5	4.50	1.70	28.9	78.4
G2	0	—	8.38	1.69	27.0	35.1
	1	-5	9.57	1.67	27.8	19.0
G3	0	—	16.12	1.65	26.0	27.4
	1	-5	16.70	1.59	27.0	11.0
F1	0	—	13.2	1.66	27.8	19.7
	3	-1	14.7	1.67	26.4	6.8
F2	0	—	11.48	1.64	29.8	16.7
	3	-5	12.60	1.55	28.4	11.8
F3	0	—	14.0	1.72	26.4	5.30
	1	-1	13.9	1.70	25.4	4.70
	3	-1	16.8	1.69	24.8	4.20
F4	0	—	8.56	1.71	29.0	21.0
	3	-1	8.99	1.67	28.6	16.1

Note: The water content and density of soil samples in Table 1 and Table 2 that fail to meet the experiment requirements and are deleted are not included in the average value of this table.

the soil sample under freeze-thaw action. The source of soil cohesion is mainly the various physical and chemical forces among soil particles, including Coulomb force, cementation force, etc., which mainly depends on the initial dry density of the soil and the mineral composition contained in the soil. In the process of freezing-thawing, the phase change of pore water can cause the compression pressure of soil particles, which destroys the original strength among soil particles and leads to the decrease of cohesion (Xu et al., 2020). The internal friction angle is mainly determined by the interlocking, mosaics and occlusions among soil particles, and the effect of freeze-thaw has little influence on them, so the internal friction angle has little change before and after freeze-thaw.

Among the existing nonlinear models, the most representative one is the Duncan-Chang hyperbolic model describing the hardening type, which is simple and intuitive with clear physical meaning of the parameters and easy to obtain directly from experiment data (Kondner, 1963; Duncan & Chang, 1970), so it is the most commonly used. Since the Duncan-Chang model cannot reflect the softening characteristics of soil, this paper only uses the test data before the peak strength to calculate the parameters of the Duncan-Chang model. Therefore, based on the experiment data, the axial deformation is taken as the abscissa, and the ratio of the axial deformation and the stress difference $\varepsilon/(\sigma_1\text{-}\sigma_3)$ is taken as the ordinate. The regression fitting of the experiment data is carried out, and the linear equations are fitted as:

$$\frac{\varepsilon}{\sigma_1-\sigma_3}=a+b\varepsilon \tag{5}$$

$$\sigma_1-\sigma_3=\frac{\varepsilon}{a+b\varepsilon} \tag{6}$$

Both a and b are experiment constants related to soil properties. According to Equation 6, the initial tangent model E_i at small strain can be obtained as:

$$E_i=\left(\frac{\sigma_1-\sigma_3}{\varepsilon}\right)_{\varepsilon\to 0}=\frac{1}{a} \tag{7}$$

When the axial strain is larger, the asymptotic value of the principal stress difference (the limit value of the stress-strain curve) is:

$$(\sigma_1-\sigma_3)_{\mathrm{ult}}=\left(\frac{\sigma_1-\sigma_3}{\varepsilon}\right)_{\varepsilon\to\infty}=\frac{1}{b} \tag{8}$$

Equation 8 is also the asymptote of the σ-ε curve. In practical engineering, the failure strength $(\sigma_1\text{-}\sigma_3)_f$ usually does not reach the asymptotic value of the principal stress difference $(\sigma_1\text{-}\sigma_3)_{ult}$ when the soil is damaged, and the ratio of the two is called the failure ratio R_f, namely:

$$R_{\mathrm{f}}=\frac{(\sigma_1-\sigma_3)_{\mathrm{f}}}{(\sigma_1-\sigma_3)_{\mathrm{ult}}} \tag{9}$$

Based on the above methods, the initial tangent modulus E_i, asymptotic values of principal stress difference $(\sigma_1\text{-}\sigma_3)_{ult}$ and failure ratio R_f of undisturbed soil samples before and after freeze-thaw under different confining pressures can be obtained, as shown in Table 4, Table 5, Table 6 and Table 7, respectively. Before and after freeze-thaw, the initial tangent modulus of the undisturbed soil sample basically shows an increasing trend with the increase of the confining pressure. Similarly, before and after freeze-thaw, the asymptotic value of the principal stress difference $(\sigma_1\text{-}\sigma_3)_{ult}$ of the undisturbed soil samples gradually increases with the increase of the confining pressure, and the asymptotic value of the principal stress difference $(\sigma_1\text{-}\sigma_3)_{ult}$ remains basically constant.

Regarding the loess failure ratio, the range of loess failure ratio studied by previous scholars is between 0.73 and 1.00 (Liu, 1997). According to Equation 9, the failure ratio of soil samples before and after the freeze-thaw cycles is estimated, and the results are listed in Table 8 and Table 9, respectively. The failure ratio of undisturbed soil samples without freeze-thaw ranges from 0.58 to 0.95, and the failure ratio of freeze-thaw soil ranges from 0.44 to 0.91. Under the same confining pressure, after freeze-thaw, the strength failure ratio of undisturbed soil samples decreases, mainly because the freeze-thaw action weakens the natural strength of the soil samples, which causes a decrease in the failure strength and eventually leads to a decrease in the failure ratio. The strength failure ratio of soil samples before and after freeze-thaw has no obvious change with the increase of confining pressure.

Table 4. E_i of soil before freeze-thaw under different confining pressures.

Confining pressure	Sample G1	Sample G2	Sample G3	Sample F1	Sample F2	Sample F3	Sample F4
(MPa)	(MPa)	(MPa)	(MPa)	(MPa)	(MPa)	(MPa)	(MPa)
0.1	34.6	12.4	10.2	6.8	7.12	1.7	8.0
0.2	46.7	15.0	13.2	10.8	18.0	8.5	—
0.3	72.8	18.8	17.7	19.8	28.7	12.7	16.1
0.4	—	14.3	19.3	—	20.6	14.7	18.5
0.5	—	12.4	19.0	—	—	—	—
0.6	—	25.6	—	—	—	—	—

Note: "—" indicates the abnormal data caused by equipment failure or sample preparation failure, not listed here.

Table 5. $(\sigma_1-\sigma_3)_{ult}$ of soil before freeze-thaw under different confining pressures.

Confining pressure (MPa)	Sample G1 (MPa)	Sample G2 (MPa)	Sample G3 (MPa)	Sample F1 (MPa)	Sample F2 (MPa)	Sample F3 (MPa)	Sample F4 (MPa)
0.1	0.45	0.29	0.23	0.22	0.21	0.20	0.24
0.2	0.73	0.46	0.45	0.51	0.58	0.45	—
0.3	1.17	0.8	0.72	0.73	0.80	0.78	0.74
0.4	—	1.66	1.17	—	1.02	0.98	1.11
0.5	—	1.83	1.41	—	—	—	—
0.6	—	1.94	—	—	—	—	—

Note: "—" indicates the abnormal data caused by equipment failure or sample preparation failure, not listed here.

Table 6. E_i and $(\sigma_1-\sigma_3)_{ult}$ of soils after freeze-thaw at a freezing temperature of -5°C.

Sample number (N)	Confining pressure (MPa)	Freezing temperature (°C)	Freeze-thaw cycle (time)	E_i (MPa)	$(\sigma_1-\sigma_3)_{ult}$ (MPa)
G1	0.1	-5	1	24.2	0.41
	0.2			44.7	0.61
	0.3			49.2	0.8
G2	0.1	-5	1	8.92	0.21
	0.2			11.6	0.44
	0.3			16.3	0.77
	0.4			18.6	1.10
	0.5			13.9	1.78
	0.6			22.7	1.83
G3	0.1	-5	1	8.60	0.20
	0.2			10.0	0.41
	0.3			11.4	0.70
	0.4			16.2	1.12
	0.5			15.2	1.44
F2	0.1	-5	3	1.16	0.18
	0.2			7.70	0.56
	0.3			12.6	0.61
	0.4			14.5	1.12

Table 7. E_i and $(\sigma_1-\sigma_3)_{ult}$ of soils after freeze-thaw at a freezing temperature of -1°C.

Sample number (N)	Confining pressure (MPa)	Freezing temperature (°C)	Freeze-thaw cycle (time)	E_i (MPa)	$(\sigma_1-\sigma_3)_{ult}$ (MPa)
F1	0.1	-1	3	1.26	0.22
	0.2			7.73	0.4
	0.3			16.4	0.71
F3	0.1	-1	3	3.22	025
	0.2			13.4	0.47
	0.3			15.5	0.67
	0.4			15.6	0.93
F4	0.1	-1	3	0.70	0.19
	0.3			9.60	0.89
	0.4			12.80	1.52

Table 8. Failure ratio of undisturbed loess before freeze-thaw.

Confining pressure	Sample G1	Sample G2	Sample G3	Sample F1	Sample F2	Sample F3	Sample F4
(MPa)	(MPa)	(MPa)	(MPa)	(MPa)	(MPa)	(MPa)	(MPa)
0.1	0.91	0.75	0.78	0.85	0.95	0.83	0.89
0.2	0.95	0.94	0.88	0.77	0.88	0.75	—
0.3	0.77	0.83	0.79	0.61	0.68	0.59	0.73
0.4	—	0.73	0.61		0.59	0.72	0.85
0.5	—	0.58	0.58		—	—	—
0.6	—	0.70	—		—	—	—

Note: "—" indicates the abnormal data caused by equipment failure or sample preparation failure, not listed here.

Table 9. Failure ratio of undisturbed loess after freeze-thaw.

Confining pressure	Sample G1	Sample G2	Sample G3	Sample F1	Sample F2	Sample F3	Sample F4
(MPa)	(MPa)	(MPa)	(MPa)	(MPa)	(MPa)	(MPa)	(MPa)
0.1	0.83	0.67	0.66	0.72	0.91	0.91	0.86
0.2	0.66	0.80	0.81	0.68	0.64	0.72	—
0.3	0.73	0.71	0.69	0.58	0.63	0.47	0.75
0.4	—	0.66	0.59		0.55	0.61	0.70
0.5	—	0.44	0.52		—	—	—
0.6	—	0.66	—		—	—	—

Note: "—" indicates the abnormal data caused by equipment failure or sample preparation failure, not listed here. Sample F3: Refers to the damage ratio after 3 freeze-thaw cycles.

4. Discussion

In this study, a total of 130 undisturbed soil samples were collected, and a small amount of soil samples were broken or cracked during transportation and sample preparation. In the process of shearing, some of the soil samples are affected by the weak surface of the original structure (such as holes or tiny cracks hidden in the soil sample, weak interlayers, and local weakness caused by uneven density, water content distribution and anisotropy) and suffer from strength failure at the initial stage of loading, so they do not meet the experiment requirements (the data are removed during the analysis). In the past, most of the studies on undisturbed soil are carried out by artificially configured parallel samples with the same water content and density indoors, and then a series of experiments are conducted to facilitate data collation and analysis, so as to get relatively consistent conclusions. In fact, due to the anisotropy, non-uniformity and non-continuity of natural soil, it is almost impossible to create parallel undisturbed soil samples with exactly the same water content and density. And through this study, it is found that due to the occurrence environment and geological origin, the physical and mechanical property of the soil has significant natural variability and randomness in the spatial distribution, resulting in larger differences in the strength, water content and density of the undisturbed soil. Moreover, the physical and mechanical property of the same soil sample in different parts are also unevenly distributed, resulting in significant differences in experiment results. In particular, it is difficult to obtain large quantities of undisturbed soil samples, which brings considerable challenges to the research work of undisturbed soil. In order to obtain the engineering mechanical parameters with practical reference value for engineering construction more systematically and comprehensively, it is necessary to carry out a large number of related experiments on the undisturbed soil, and provide more accurate and reliable relevant parameters for engineering construction by means of probability theory, mathematical statistics and neural network. In addition, the variability of soil parameters is characterized by the coexistence of structure and randomness, and it is more reasonable to deal with it by random field theory.

5. Conclusion

1. The mechanical properties of undisturbed loess are greatly affected by freeze-thaw, water content, natural density and confining pressure. Before and after freeze-thaw, the shape of the shear failure surface is complex, including single oblique failure surface, double oblique failure surface, vertical failure surface, X-shaped failure surface, bulging failure.
2. Freeze-thaw, water content, dry density and confining pressure have great influence on the stress-strain curve. Before and after freeze-thaw, the stress-strain curve tends to be softening type under low water content, low confining pressure and high dry density. Otherwise, the curve tends to be hardening type. And freeze-thaw action can make the stress-strain curve transition from softening to hardening.

3. Repeated freeze-thaw action weakens the shear strength, cohesion, initial tangent modulus, the asymptotic value of the principal stress and the failure ratio of undisturbed soil, but the internal friction angle does not change significantly.

Acknowledgements

This study was funded by the National Natural Science Foundation of China (grant number 51769013; 52168052) and China Energy Construction Group Gansu Electric Power Design Institute Co., LTD. Science and Technology Project.

Declaration of interest

The authors have no conflicts of interest to declare. All co-authors have observed and affirmed the contents of the paper and there is no financial interest to report.

Authors' contributions

Shuangshuang Yang: experiment, data curation. Yaling Chou: conceptualization, methodology, idea, validation. Lijie Wang: investigation, writing – original draft preparation, modeling. Peng Zhang: writing – reviewing & editing, language.

Data availability

The datasets generated analyzed in the course of the current study are available from the corresponding author upon request.

List of symbols

a	intercept of failure principal stress line and q-axis
c	cohesion
E_i	initial tangent model
R_f	movements of the pile top (Bidirectional test)
α	the inclination of the failure principal stress line and the p-axis
σ_1	maximum effective principal stresses
σ_3	minimum effective principal stresses
$(\sigma_1\text{-}\sigma_3)_{ult}$	the asymptotic value of the principal stress difference
φ	internal friction angle

References

Bjerrum, L. (1967). Engineering geology of Norwegian normally-consolidated marine clays as related to settlements of buildings. *Geotechnique*, *17*(2), 83-118. http://dx.doi.org/10.1680/geot.1967.17.2.83.

Burland, J.B. (1990). Thirtieth Rankine Lecture-on the compressibility and shear strength of natural clays. *Geotechnique*, *40*(3), 329-378. http://dx.doi.org/10.1016/0148-9062(91)92860-2.

Chamberlain, E.J., & Gow, A.J. (1979). Effect of freezing and thawing on the permeability and structure of soils. *Engineering Geology*, *13*(1-4), 73-92. http://dx.doi.org/10.1016/0148-9062(79)91523-7.

Dong, X.H., Zhang, A.J., Lian, J.B., & Guo, M.X. (2010a). Study of shear strength deterioration of loess under repeated freezing-thawing cycles. *Journal of Glaciology and Geocryology*, *32*(4), 767-772.

Dong, X.H., Zhang, A.J., Lian, J.B., & Guo, M.X. (2010b). Laboratory study on shear strength deterioration of loess with long-term freezing-thawing cycles. *Journal of Engineering Geology*, *18*(6), 887-893. http://dx.doi.org/10.3969/j.issn.1004-9665.2010.06.012.

Duncan, J.M., & Chang, C.Y. (1970). Nonlinear analysis of stress and strain in soils. *Journal of the Soil Mechanics and Foundations Division*, *96*(5), 1629-1653. http://dx.doi.org/10.1061/JSFEAQ.0001458.

Fang, L.L., Qi, J.L., & Ma, W. (2012). Freeze-thaw induced changes in soil structure and its relationship with variations in strength. *Journal of Glaciology and Geocryology*, *34*(2), 435-440.

Hu, Z.Q., Liu, Y., & Li, H.R. (2014). Influence of freezing-thawing cycles on strength of loess. *Journal of Hydraulic Engineering*, *45*(S2), 14-18. http://dx.doi.org/10.13243/j.cnki.slxb.2014.S2.003.

Kondner, R.L. (1963). Hyperbolic stress-strain response: cohesive soils. *Journal of the Soil Mechanics and Foundations Division*, *89*(1), 115-143. http://dx.doi.org/10.1061/JSFEAQ.0000479.

Konrad, J.M. (1989). Physical processes during freeze-thaw cycles in clayey silts. *Cold Regions Science and Technology*, *16*(3), 291-303. http://dx.doi.org/10.1016/0165-232X(89)90029-3.

Li, S.H., Li, Y.X., Gao, X.Y., & Shi, D.M. (2020). Effect of freezing and thawing on shear strength of intact loess. *Journal of Civil and Environmental Engineering*, *42*(1), 48-55. http://dx.doi.org/10.11835/j.issn.2096-6717.2019.145.

Liu, Z.D. (1997). *Loess mechanics and engineering*. Xian: Shanxi Science and Technology Press.

Ma, W., Xu, X.Z., & Zhang, L.X. (1999). Influence of frost and thaw cycles on shear strength of lime silt. *Chinese Journal of Geotechnical Engineering*, *21*(2), 158-160. http://dx.doi.org/10.3321/j.issn:1000-4548.1999.02.005.

Ni, W.K., & Shi, H.Q. (2014). Influence of freezing-thawing cycles on micro-structure and shear strength of loess. *Journal of Glaciology and Geocryology*, *36*(4), 922-927. http://dx.doi.org/10.7522/j.issn.1000-0240.2014.0111.

Qi, J.L., Zhang, J.M., & Zhu, Y.L. (2003). Influence of freezing-thawing on soil structure and its soil mechanics significance. *Chinese Journal of Rock Mechanics and*

Engineering, *22*(S2), 2690-2694. http://dx.doi.org/10.3321/j.issn:1000-6915.2003.z2.032.

She, H.C., Hu, Z.Q., Xue, T., Zhang, R.J., Li, L., & He, M.M. (2020). Structural strength deterioration characteristics of undisturbed loess by moistening and freezing-thawing. *Kexue Jishu Yu Gongcheng*, *20*(4), 1558-1566. http://dx.doi.org/10.3969/j.issn.1671-1815.2020.04.040.

Song, C.X., Qi, J.L., & Liu, F.Y. (2008). Influence of freeze-thaw on mechanical properties of Lanzhou loess. *Rock and Soil Mechanics*, *29*(4), 1077-1080. https://doi.org/10.3969/j.issn.1000-7598.2008.04.042.

Wang, D.Y., Ma, W., Chang, X.X., Sun, Z.Z., Feng, W.J., & Zhang, J.W. (2005). Physico-mechanical properties changes of Qinghai-Tibet clay due to cyclic freezing and thawing. *Chinese Journal of Rock Mechanics and Engineering*, *24*(23), 4313-4319. http://dx.doi.org/10.3321/j.issn:1000-6915.2005.23.018.

Wang, D.Y., Ma, W., Niu, Y.H., & Xiao, X. (2007). Effects of cyclic freezing and thawing on mechanical properties of Qinghai-Tibet clay. *Cold Regions Science and Technology*, *48*(1), 34-43. http://dx.doi.org/10.1016/j.coldregions.2006.09.008.

Wang, T.H., Luo, S.F., & Liu, X.J. (2010). Testing study of freezing-thawing strength of unsaturated undisturbed loess considering influence of moisture content. *Yantu Lixue*, *31*(8), 2378-2382. http://dx.doi.org/10.3969/j.issn.1000-7598.2010.08.005.

Wei, Y., Yang, G.S., & Ye, W.J. (2018). Impact of freezing temperature on mechanical properties of loess under cyclic freezing and thawing. *Changjiang Kexueyuan Yuanbao*, *35*(8), 61-66. http://dx.doi.org/10.11988/ckyyb.20170188.

Xu, J., Li, C.Y., Wang, Z.Q., Ren, J.W., & Yuan, J. (2016). Experimental analysis on the mechanism of shear strength deterioration of undisturbed loess during the freeze-thaw. *Journal of Civil and Environmental Engineering*, *38*(5), 90-98. http://dx.doi.org/10.11835/j.issn.1674-4764.2016.05.012.

Xu, J., Zhang, M.H., Li, Y.F., & Wu, Z.P. (2020). Experimental study on deterioration behavior of saline undisturbed loess with sodium sulphate under freeze-thaw action. *Chinese Journal of Geotechnical Engineering*, *42*(9), 1642-1650. http://dx.doi.org/10.11779/CJGE202009008.

Xu, X.Z., Wang, J.C., & Zhang, L.X. (2001). *Physics of frozen soil*. Beijing: Science Press.

Yang, C.S., He, P., Cheng, G.D., Zhu, Y.L., & Zhao, S.P. (2003). Testing study on influence of freezing and thawing on dry density and water content of soil. *Chinese Journal of Rock Mechanics and Engineering*, *22*(S2), 2695-2699. http://dx.doi.org/10.3321/j.issn:1000-6915.2003.z2.033.

Ye, W.J., Liu, K., Yang, G.S., Ma, W.C., & Xie, Z.W. (2018). Experimental study on shear strength deterioration of loess under freeze-thaw cycling. *Kexue Jishu Yu Gongcheng*, *18*(3), 313-318. http://dx.doi.org/10.3969/j.issn.1671-1815.2018.03.051.

Ye, W.J., Yang, G.S., Peng, J.B., Huang, Q.B., & Xu, Y.F. (2012). Test research on mechanism of freezing and thawing cycle resulting in loess slope spalling hazards in LuoChuan. *Chinese Journal of Rock Mechanics and Engineering*, *31*(1), 199-205. http://dx.doi.org/10.3969/j.issn.1000-6915.2012.01.023.

Zhu, L.N. (1988). Study of the adherent layer on different types of ground in permafrost regions on the Qinghai-Xizang Plateau. *Journal of Glaciology and Geocryology*, *10*(1), 8-14.